Journal of Applied Mechanics and Technical Physics, Vol. 43, No. 4, pp. 630–637, 2002

FRACTURE OF SPHEROPLAST SAMPLES WITH DIFFERENT TYPES OF STRESS CONCENTRATORS

E. V. Karpov

UDC 539.3

The paper reports results of experimental studies of stress concentration in cylindrical samples of spheroplasts (composites in which the binder is dianepoxy and the filler is glass microspheres) with some types of concentrators and fracture of these samples under uniaxial compression. We performed numerical modeling of the stress–strain state of homogeneous samples with concentrators in a static, linearly elastic formulation and modeling of the effects due to fracture of the samples.

Description of Samples, Materials, and Experimental Conditions. We studied samples of ÉDS-7 and ÉDS-5A spheroplasts — composites consisting of dianepoxy (ÉDS-5A also contains a plastifier) and a filler in the form of glass microspheres (microcapsules) [1–3]. Most of the microspheres have diameter of 10 to 40 μm, and the walls of the microspheres are 1–2 μm thick. The numeral in the name of a spheroplast denotes the density of the material. Thus, the density of ÉDS-7 samples is about 0.7 g/cm^3. In experiments on compression of cylinders and bars without concentrators, the Young's modulus is 2800 MPa for a ÉDS-7 and 1600 MPa for ÉDS-5A, and the Poisson's ratio ν obtained in the same experiments is 0.3 for both materials.

The samples were circular cylinders 167 mm long and 45 mm in diameter with transverse cylindrical holes of radius 5 and 8 mm, respectively (Fig. 1). We also tested a bar 167 mm long which had a square cross section with side 45 mm long, a cylindrical sample with a hole of 5 mm radius reinforced by a rigid insert, and cylindrical samples of various dimensions without holes. All samples were loaded by a compressive force directed along the Z axis (Fig. 1). Before crack nucleation (the moment of nucleation was determined by a characteristic noise), the samples were subjected to a series of identical loading under static conditions and the strains ε_{ZZ} were measured by foil strain gauges located on the longitudinal axis a and the transverse arc b (Fig. 1) at various distances from the hole (measurement results are given below). Then, the samples were fractured by uniaxial compression.

Fracture Experiments. A series of experiments was performed on fracture of spheroplast cylinders with some types of concentrators. Photographs of the fractured samples are shown in Fig. 2. Sample Nos. 1 and 2 were made of ÉDS-5A and have holes of radii 5 and 8 mm, respectively. Sample No. 3 was made of ÉDS-7 and had a hole of 5 mm radius. Sample No. 4 made of ÉDS-5A had square cross section and a hole of 5 mm radius. Sample Nos. 5 and 6 made of ÉDS-5A had no holes. Sample 7 was made of ÉDS-5A and had a hole of 5 mm radius reinforced by a rigid insert.

All samples fractured with formation of a crack lying in the plane of the diametral section XZ. The crack side had the shape of even flat surfaces. In sample Nos. 1–4, after the crack had propagated over the entire sample, parts of the samples broke in the transverse direction near the hole with spallation of rather large pieces of the material near the concentrator (sample Nos. 3 and 4) or the butts (sample Nos. 1 and 2). In sample No. 7, instead of the transverse break of the parts there was cleavage at an angle close to 45°.

When the hole was not reinforced by a rigid insert, longitudinal fracture of the sample was caused by the concentration of tensile stresses σ_{YY} in the plane XZ near the hole. Here fracture occurs jumpwise. For ÉDS-5A samples, crack opening (up to 5 mm at the wide end) with jumpwise propagation to the butts was observed. After formation of an open crack, the load did not change during further compression up to complete fracture. In ÉDS-7 samples, the crack remained open up to the moment of complete fracture under increasing loading.

Lavrent'ev Institute of Hydrodynamics, Siberian Division, Russian Academy of Sciences, Novosibirsk 630090.
Translated from Prikladnaya Mekhanika i Tekhnicheskaya Fizika, Vol. 43, No. 4, pp. 170–179, July–August, 2002. Original article submitted December 28, 2001; revision submitted March 4, 2002.

 0021-8944/02/4304-0630 $27.00

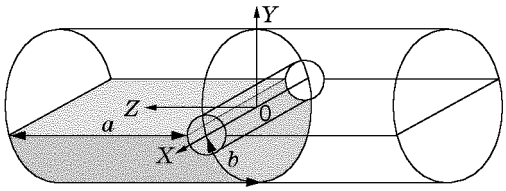

Fig. 1

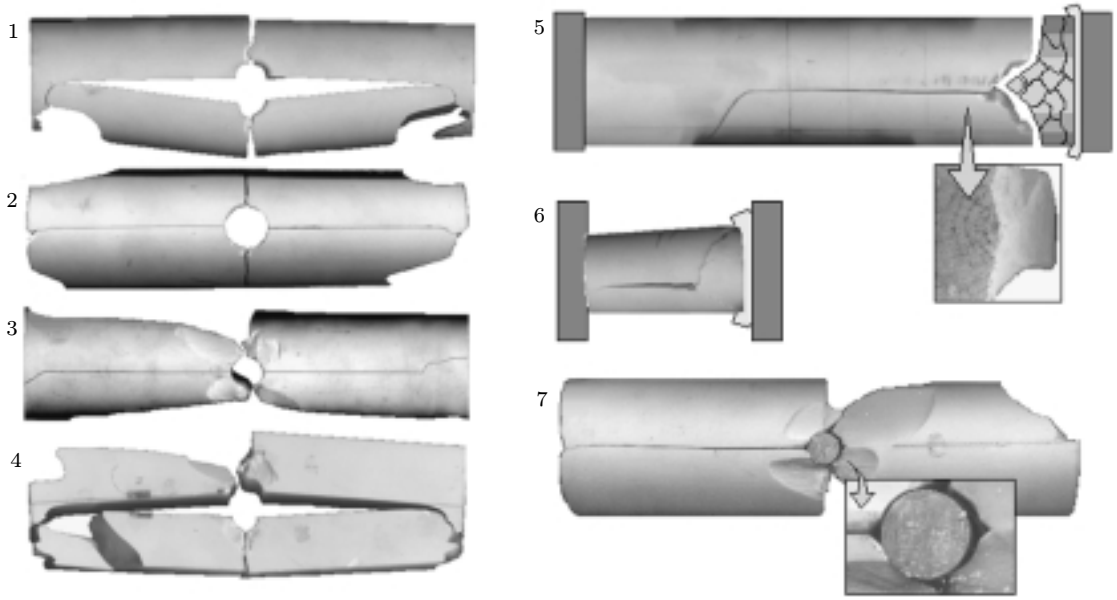

Fig. 2

In sample Nos. 5 and 6, the left butt was in direct contact to the mold anvil, and at the right butt, a fluoroplastic insert was placed between the sample and the anvil. In these samples, a fractured wedge-shaped region formed at the butt with the fluoroplastic insert, after which the remaining part of the sample split along the plane of symmetry (for sample No. 5, the wedge-shaped part is shown schematically because it was broken into a large number of small fragments as a result of fracture). After formation of the wedge-shaped region, the tensile stresses σ_{YY} concentrated in the corner of the curved leading edge of the wedge, which is shown near the fractured butt of sample No. 5 on the part of a photograph of the fracture surface in Fig. 2.

In the case of a hole reinforced by an insert, fracture proceeded in two stages. Initially, compressive stresses σ_{ZZ} led to local fracture of microspheres and compaction of the porous material in the concentration zones. The material, remaining elastic in compression, ceased to resist to fracture, which led to the formation of two additional concentrators. In Fig. 2 (enlarged fragment of sample No. 7) they have the shape of triangular holes on each side of the insert. These concentrators caused a sudden jump of the tensile stresses σ_{YY} in the plane XZ near the hole, which led to fast fracture in the plane XZ.

In sample Nos. 1 and 3–6, the fracture surfaces show a characteristic relief (Fig. 3) which consists of a region convex toward the butt and adjacent to the concentrator edge (in Fig. 3, the black region near the left edge of the fracture surface), and curved narrow relief strips of identical curvature, which crowd together approaching the butt. The relief is symmetric about the concentrator (for samples with a hole). Upon superimposition for identical samples, the reliefs on the fracture surface coincide with accuracy up to the width of the curved strips. For samples of identical geometry made of different materials, the reliefs differ only in the distance from the first curved strip to the concentrator. The presence of this relief is characteristic of samples of both round and square cross sections. For different geometries (different types of concentrator or different midsection areas) there are differences in the curvature of the relief strips, their concentration, characteristic dimensions of the relief, and remoteness of the first strip from the concentrator.

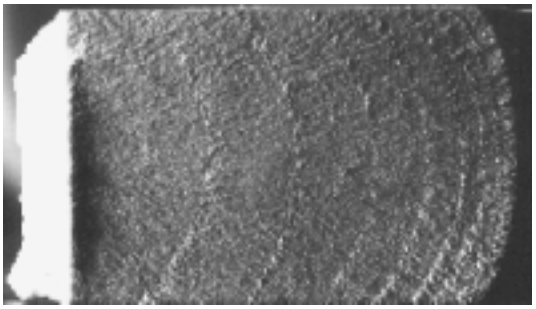

Fig. 3

A relief on the fracture surface was not observed in the case of fast fracture caused by a sudden change of tensile stresses (reinforced hole), and in the case of a great hole radius (8 mm), where the primary crack immediately passed through almost the entire sample and stopped at about 10 mm from the butts.

A LEO-420 scanning electron microscope was used to take photographs of the material structure in various regions of the smooth fracture surface between the relief strips, on the strips, and in the relief zone adjacent to the concentrator. The microscopic study showed that besides the distinct relief, there is one more feature that distinguishes the curved strips and the convex zone adjoining the concentrator edge from the remaining surface. On the curved strips and in the convex zone, the microspheres are broken, whereas on the remaining part of the surface, they are intact.

The wholeness of the microspheres on the fracture surface indicates that the fracture occurred by normal separation because shear fracture would have cut off the spheres.

Comparison of Numerical Results with Experimental Data. Numerical experiments were performed to model the stress–strain states in the samples examined.

Problems of axial compression in a static, linearly elastic formulation were solved by the finite-element method. Models were constructed using three-dimensional, isoparametric, eight-nodal final elements. The material was considered homogeneous. The calculations were performed at the Center of Computer Technologies in Mechanics (Institute of Mechanics of the Moscow State University) using the ANSYS finite-element code.

A comparison of experimental data and calculation results is given in Fig. 4. Figure 4a shows curves of the nondimensional coefficient $\varepsilon_{ZZ}E/\sigma$ versus the applied stress σ (E is the Young's modulus of the spheroplast and ε_{ZZ} is the strain measured by the gauge). The coefficient $\varepsilon_{ZZ}E/\sigma$ is the ratio of the strain ε_{ZZ} to the strain corresponding to the stress σ in an elastic flawless spheroplast with Young's modulus E. In the case of $\varepsilon_{ZZ}E/\sigma > 1$, this quantity is called the stress concentration coefficient σ_{ZZ}. Figure 4a gives data for a ÉDS-7 sample with a hole radius of 5 mm (for the remaining samples, the data are similar). The figure shows sets of experimental points for each of the gauges available on the sample and values of the coefficient $\varepsilon_{ZZ}E/\sigma$ for the calculated values of ε_{ZZ} at the locations of the gauges. The calculated values of the coefficient $\varepsilon_{ZZ}E/\sigma$ do not depend on the value of the applied load. These values are inside horizontal strips of various width, whose top and bottom boundaries correspond to the largest and smallest values of $\varepsilon_{ZZ}E/\sigma$ within the area occupied up by the gauge. The calculated values and sets of experimental points correspond to the gauge numbers. Gauge Nos. 1 and 3 are located on the longitudinal axis a (see Fig. 1) at a distance of 2 mm from the hole edge (symmetric about the center of the hole), and gauge Nos. 6 and 7 are placed on the longitudinal axis a at 6 and 30 mm from the hole edge, respectively. Gauge Nos. 2 and 4 are located on the transverse arc b at 2 mm from the hole edge (asymmetrically about the center of the hole), and gauge Nos. 5 and 8 are located on the transverse arc b at 6 and 32 mm from hole edge, respectively.

In Fig. 4 it is evident that at the beginning of loading, large jumps of strains are observed at the locations of almost all gauges (in the less dense material ÉDS-5A, at the locations of all gauges). With further loading, the coefficient $\varepsilon_{ZZ}E/\sigma$ practically ceases to depend on the applied stress, i.e., linearly-elastic deformation occurs. The initial jumps are most likely a consequence of the initial stabilization of the sample, which, as a rule, is observed at the first stage of loading in experiments. Therefore, in deriving the mean experimental coefficient for comparison with the calculated value, we take into account only the stage of stable deformation.

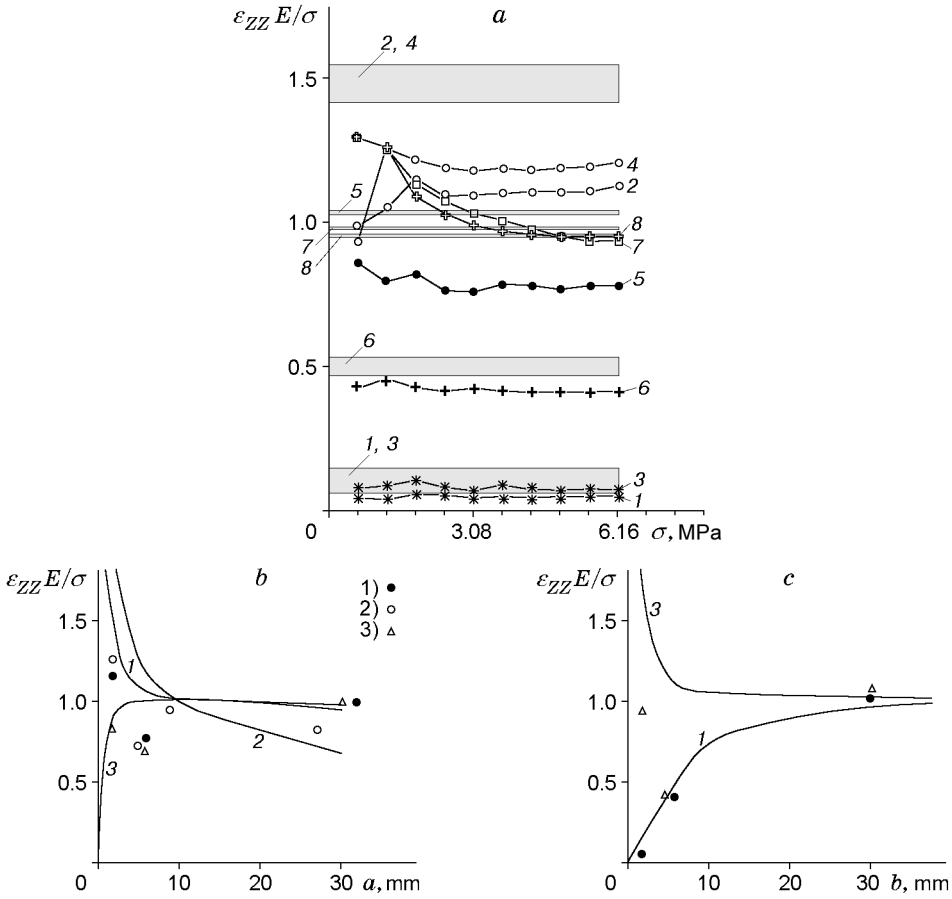

Fig. 4

A comparison with calculation results shows the following. For the gauges located in the zones where $\varepsilon_{ZZ}E/\sigma < 1$, the experimental strains are close to the values calculated by the finite-element model. At the same time, the gauges located in the calculation zone of stress concentration detect strains much smaller than the calculated values. This decrease of strains is clearly seen on the curves shown in Fig. 4b and c. This figure gives curves of the coefficient $\varepsilon_{ZZ}E/\sigma$ versus the coordinates on the transverse arc b and the longitudinal axis a reckoned from the hole edges. Points 1 correspond to the sample with a hole radius of 5 mm, points 2 to the sample with a hole radius of 8 mm, and points 3 to the sample with a hole radius of 5 mm reinforced by a rigid insert. Curves 1–3 are calculated dependences for the corresponding samples. In Fig. 4b and c it is evident that in the concentration zones there is a strong decrease of strains relative to calculated values. Moreover, instead of decreasing monotonically with distance from the hole, the strain decreases abruptly near the concentrator edges and then increases to average values over the sample. For the sample with a rigid insert, this effect is observed near the hole on both the longitudinal axis, where there is stress concentration, and on the transverse arc, where the stress is lower than that applied at the butts.

A possible cause of the decrease of strains in the stress concentration zones is as follows. Near the sample surface formed by drilling the hole there is a thin cylindrical layer of the material with broken microspheres. In the zones of the highest concentration of compressive stresses there may be local collapse of the spheroplast weakened by fracture of part of the microspheres. Collapse of spherical hollows makes the material more rigid, which should result in a decrease of strain near the local fracture zone. Further propagation of the local fracture zone into the depth of the material is also possible. For ÉDS-5A samples, such propagation is suggested by the fact that for some gauges located in the concentration zones there is no horizontal segment on the experimental curves of the coefficient $\varepsilon_{ZZ}E/\sigma$ versus the edge stress.

A calculation was performed of the stress–strain state with a local increase of Young's modulus in the region of the highest concentration of compressive stresses. Results of the calculation do not contradict results of the

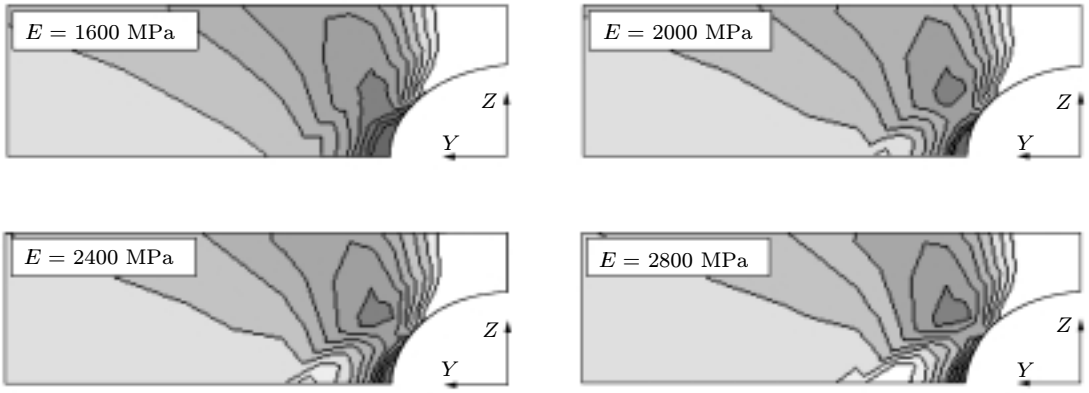

Fig. 5

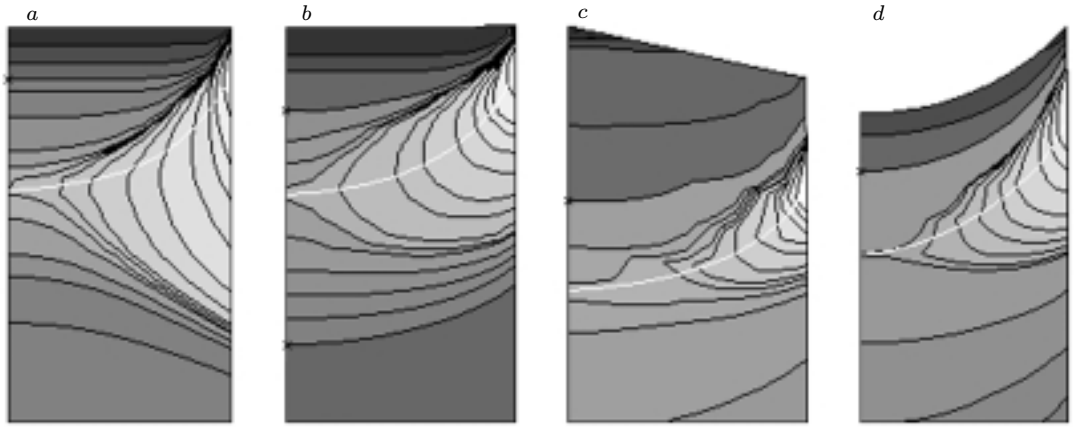

Fig. 6

experiments, in which the occurrence of zones of decreased strain was observed. Figure 5 gives fields of compressive strains ε_{ZZ} for various values of Young's modulus in the concentration zone. Light regions correspond to smaller strains, and dark regions to large strains.

When the stresses applied at the butts are close to the critical stresses resulting in crack nucleation in the plane XZ, the process observed in the concentration zones is similar to that which is likely to lead to the occurrence of the regions of decreased strains described above. There is spontaneous increase of strain without increase of applied stress. After that, the dependence of strain on applied stress becomes linear again, and the stiffness of the material increases compared to the original value.

Figure 6 shows fields of stresses σ_{YY} in the plane of fracture XZ. Calculation results for the cylinder and the bar with a transverse hole are shown in Fig. 6a and b, and calculation results for the case where there is a broken wedge-shaped part near one butt are given in Fig. 6c. The action of this part is replaced by the action of compressive stresses normal to the surfaces on which the wedge-shaped part is separated from the remaining sample. Figure 6d gives calculation results for a cylinder in which, besides the transverse hole, there is a crack in the plane XZ which propagates from the hole edges and has the leading edge coincident with the first curved relief strip for ÉDS-7 samples (see Fig. 3). In Fig. 6a–d, the concentrator edge is located at the top of the figure, the line of intersection of the fracture surface with the sample surface is on the right, and the symmetry axis Z is on the left. The butt toward which the crack propagated in the experiments is located outside Fig. 6 (below). The Y axis is perpendicular to the plane of the figure. In the case shown in Fig. 6 there are both tensile and compressive stresses. Crosses show the boundary between them (isoline of zero stresses). The lightest regions correspond to the highest compressive stresses, and the darkest regions correspond to tensile stresses. The values of stresses corresponding to the isolines are not given because experimental determination of stresses inside an intact sample seems impossible.

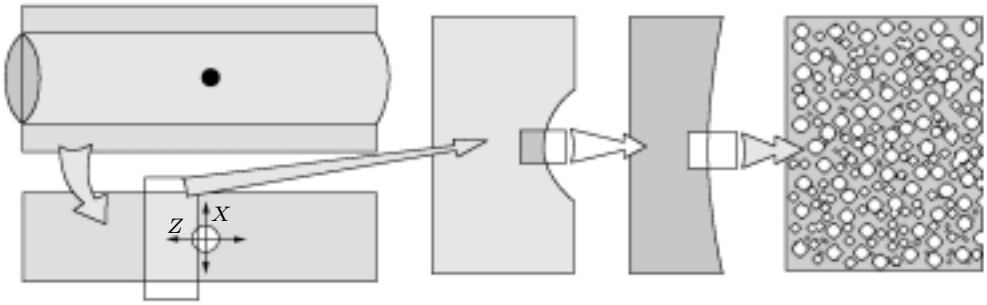

Fig. 7

Comparison of calculated stress fields σ_{YY} in the plane of fracture with results of fracture of the samples showed the following. For all types of concentrators considered, which directly lead to crack formation in the plane XZ (a hole without an insert, a hole and a crack with curved edge, a sample with broken wedge-shape part), the same type of stress distribution is observed (Fig. 6). Near the concentrator there is a zone of tensile stresses which is convex toward the butt. Ahead of this zone, zones of compressive stresses form. The points at which the isolines of compressive stresses have the least curvature are located along a certain curve (white curve in Fig. 6). Compressive stresses are distributed along this curve so that at the ends, they are maximal and decrease with approach to the symmetry axis, retaining nonzero values. The shapes of these curves and the shapes of the curved relief strips (see Fig. 3) are identical, which is valid for all types of sample geometry considered. In addition, the relief strips on the fracture surface are similar in shape and dimensions to the calculated zone of dangerous tensile stress concentration in the case where the concentrator includes a crack with a curved leading edge. This suggests that exactly the presence of the compression zones described above is responsible for crack retardation and arrest, and the curved relief strips are the leading edges of the crack at the moments of stops. The zone of primary crack nucleation at the hole edges is the relief convex zone adjacent to the hole, which is also similar in dimensions and shape to the dangerous concentration zone.

Model of Crack Nucleation at the Spheroplast's Structure Level. It is shown experimentally that the zone convex toward the butt and adjacent to the concentrator and the curved strips differ from the total fracture surface in the presence of a distinct relief and broken microspheres. Calculations for the model for a homogeneous material show that in the plane XZ, only tensile stresses σ_{YY} reach dangerous values, and, therefore, only these stresses can be responsible for the fracture of the microspheres and occurrence of a relief.

The difference of the relief zones from the remaining surface can be explained if from the macroscopic level we go over to the level of structure of the spheroplast. Possibly, the formation of a macroscopic crack is preceded by nucleation of a set of microcracks in the matrix between the spherical inserts, from which the main crack is then formed. Since the structure of the spheroplast is disordered, propagation of microcracks in different directions is possible at this stage. This should cause random redistribution of the centers of concentration of tensile stress σ_{YY}, which can lead to distortion and fracture of microspheres and to formation of a relief on the macroscopic fracture surface. Such process can occur in the relief zone adjacent to edge of the cylindrical concentrator, where crack nucleation occurs in the plane XZ. The same process occurs in the curved relief strips, in which there is transition from the stationary state of the main crack to further propagation.

To clarify the crack nucleation mechanism at the level of structure of the spheroplast, we constructed a finite element model. The region of the sample whose stress–strain state was modeled is shown in Fig. 7. This is a flat plate which belongs to the section of the sample by a plane parallel to YZ. One side of the plate belongs to the edge of the hole. Figure 8 gives a finite-element model of this plate (the side belonging to the edge of the concentrator faces downward) composed of fragments shown in Fig. 8a (the elements of dark color are glass rings which sections of the microspheres are made, and the lighter elements are epoxy). The boundary conditions are shown schematically in Fig. 8b: the plate is rigidly fixed from above, and tensile stresses decreasing with distance from the free lower edge are applied on each side. Fracture was modeled by removal of the set of finite elements in which dangerous values of the tensile stresses were detected. A deformed glass ring was considered broken if on one of its segments, the curvature radius became much less than the mean value. The modeling result is shown in Fig. 9, which give different stages of fracture. The dark zones denoted by arrows correspond to elevated fracture stresses.

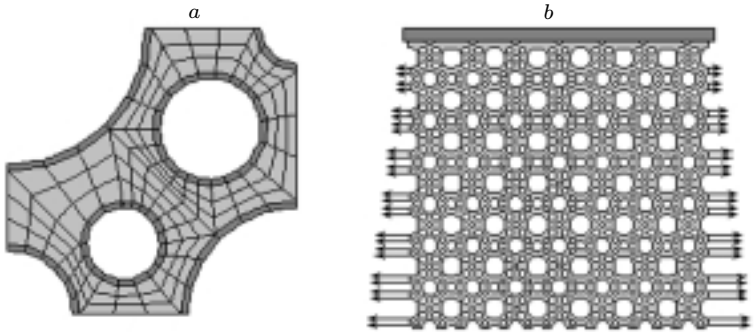

Fig. 8

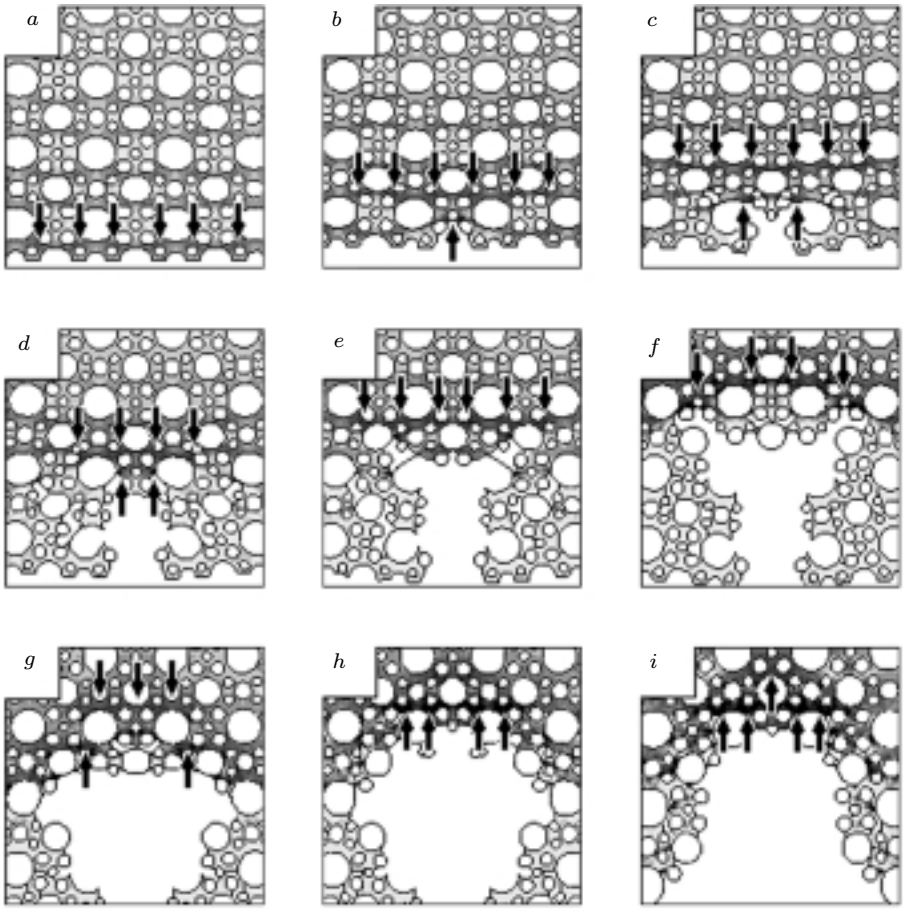

Fig. 9

The numerical modeling yields the following picture of crack nucleation in the structure of the spheroplast. Prior to the beginning of fracture, identical centers of dangerous stresses are distributed over the entire free boundary (Fig. 9a). Therefore, primary fracture can occur in any place of the boundary where any microdefect appears. Consequently, in neighboring planes, fracture occur in different places, which may be responsible for relief formation. When a primary fracture appears, a front of identical spots of elevated stresses arises ahead of it, and these stresses are higher than those on the free boundary prior to the fracture (Fig. 9b). Because the maximum stresses in these spots are identical, the material ahead of the primary fracture begins to crack, which leads to distortion and break of the glass rings (Fig. 9c). As the cracking zone extends (Fig. 9d–f) and propagates into the depth of the material, the stresses in the spots of the front grow. This growth is faster near the middle of the front than on the edges. When the difference reaches a certain limit after which fracture in the extreme spots is preceded by fracture in

the spots located near the center, the front and the cracking zone begin to narrow. As a result, a wedge of spots of high fracture stresses (Fig. 9g–i) forms ahead of the crack. After formation of the wedge, the random cracking ceases because the stresses in the wedge predominate over all neighboring stresses. Thus, a main crack arises, whose propagation is accompanied by the formation of two surfaces without a considerable relief and fracture of the rings. The chipping of the material in the cracking zone, whose dimensions are much larger than the effective diameter of the microspheres even in the symmetric model, leads to the formation of a relief, which confirms the above assumptions on the nature of the relief, observed on the fracture surfaces.

When the main crack forms not at the hole edges but inside a curved strip, the free boundary is much less but in this case, too, a front of spots of identical dangerous stresses forms ahead of the primary fracture. This leads to random cracking, which is responsible for fracture of the microspheres and relief formation.

Conclusions. A series of experiments was performed on uniaxial compression fracture of cylindrical spheroplast samples of circular cross sections and a bar of square cross section with some types of stress concentrators. Effects due to distinguishing features of a porous reinforced structure of the spheroplast are detected at the stage of general elastic deformation (local fracture of the structure near the concentrator) and at the stage of fracture of the samples (formation of smooth surfaces of normal fracture with a relief zone convex toward the butt and adjacent to the concentrator edge, and a number of curved relief strips, which crowd together with approach to the butts of the samples). The experimental data, microscopic investigation of the structure, and numerical experiments suggest a hypothesis on crack nucleation and propagation in a cylindrical spheroplast sample with a concentrator.

The author thanks M. P. Bondar', A. G. Demeshkin, Ya. L. Luk'yanov, and P. A. Mossakovskii.

REFERENCES

1. A. A. Berlin and F. A. Shutov, *Hardened Gas-Filled Plastic* [in Russian], Khimiya, Moscow (1980).
2. P. G. Krzhechkovskii, "Determining the elastic and strength properties of a composite material based on hollow spherical inserts," *Probl. Prochn.*, No. 3, 37–40 (1979).
3. P. G. Krzhechkovskii, "Mechanics of fracture of spheroplasts," *Probl. Prochn.*, No. 11, 110–115 (1982).